Biochimica et Biophysica Acta 1808 (2011) 164–170

Contents lists available at ScienceDirect

Biochimica et Biophysica Acta

journal homepage: www.elsevier.com/locate/bbamem

Multiple stages of detergent-erythrocyte membrane interaction—A spin label study

Paulo S.C. Preté [a], Cleyton C. Domingues [a], Nilce C. Meirelles [a], Sônia V.P. Malheiros [b], Félix M. Goñi [c], Eneida de Paula [a,*], Shirley Schreier [d]

[a] Department of Biochemistry, Institute of Biology, State University of Campinas, SP, Brazil
[b] Department of Biology and Physiology, Faculty of Medicine of Jundiaí, SP, Brazil
[c] Biophysics Unit (CSIC-UPV/EHU) and Department of Biochemistry, Universidad del País Vasco, 48080 Bilbao, Spain
[d] Department of Biochemistry, Institute of Chemistry, University of São Paulo, SP, Brazil

ARTICLE INFO

Article history:
Received 30 April 2010
Received in revised form 15 September 2010
Accepted 26 October 2010
Available online 29 October 2010

Keywords:
Erythrocyte
Membrane
Solubilization
Triton X-100
Hemolysis
EPR

ABSTRACT

The various stages of the interaction between the detergent Triton X-100 (TTX-100) and membranes of whole red blood cells (RBC) were investigated in a broad range of detergent concentrations. The interaction was monitored by RBC hemolysis–assessed by release of intracellular hemoglobin (Hb) and inorganic phosphate–and by analysis of EPR spectra of a fatty acid spin probe intercalated in whole RBC suspensions, as well as pellets and supernatants obtained upon centrifugation of detergent-treated cells. Hemolysis finished at *ca.* 0.9 mM TTX-100. Spectral analysis and calculation of order parameters (*S*) indicated that a complex sequence of events takes place, and allowed the characterization of various structures formed in the different stages of detergent–membrane interaction. Upon reaching the end of cell lysis, essentially no pellet was detected, the remaining EPR signal being found almost entirely in the supernatants. Calculated order parameters revealed that whole RBC suspensions, pellets, and supernatants possessed a similar degree of molecular packing, which decreased to a small extent up to 2.5 mM detergent. Between 3.2 and 10 mM TTX-100, a steep decrease in *S* was observed for both whole RBC suspensions and supernatants. Above 10 mM detergent, *S* decreased in a less pronounced manner and the EPR spectra approached that of pure TTX-100 micelles. The data were interpreted in terms of the following events: at the lower detergent concentrations, an increase in membrane permeability occurs; the end of hemolysis coincides with the lack of pellet upon centrifugation. Up to 2.5 mM TTX-100 the supernatants consist of a (very likely) heterogeneous population of membrane fragments with molecular packing similar to that of whole cells. As the detergent concentration increases, mixed micelles are formed containing lipid and/or protein, approaching the packing found in pure TTX-100 micelles. This analysis is in agreement with the models proposed by Lasch (Biochim. Biophys Acta 1241 (1995) 269-292) and by Le Maire and coworkers (Biochim. Biophys. Acta 1508 (2000) 86-111).

1. Introduction

Detergents are amphiphilic molecules able to wet surfaces, penetrate soil and solubilize fatty materials. Moreover, they have microbicidal effects and are widely used to solubilize membrane components, in particular proteins [1–3].

The interest in detergent–membrane interaction concerns also the physico-chemical and molecular aspects of this interaction. One interesting aspect is the interplay between bilayer and micellar structure as a function of lipid and detergent concentration, as well as their molar ratios. Theoretical and experimental work has shown that several steps take place during lipid bilayer-detergent interaction to disrupt the membrane. Different models have been proposed for the events that occur during the process of membrane solubilization. In the model of Lichtenberg et al. three main stages can be envisioned: (i) at low detergent concentration and low detergent:lipid molar ratios (D/L), molecules of the detergent are inserted into the lipid bilayer, until a limiting saturation concentration, C^{sat}, is reached. (ii) Subsequently, lipids are extracted from the bilayer by already formed micelles, giving rise to the coexistence of detergent-containing bilayers and lipid-containing micelles. (iii) As the detergent concentration increases further, total bilayer solubilization occurs (at a particular detergent concentration, C^{sol}). Further detergent addition leads to micelles with increasing D/L [4]. Lasch [5] has described the process of membrane–detergent interaction as consisting of four stages, namely, (i) detergent intercalation in the membrane, (ii) coexistence between mixed bilayer vesicles and mixed bilayer sheets, (iii) transition from mixed bilayers to lipid-rich mixed micelles and (iv) decrease in particle size, as far as

Abbreviations: CMC, critical micelle concentration; EPR, electron paramagnetic resonance; Hb, hemoglobin; Ht, hematocrit; PBS, phosphate buffered saline; RBC, red blood cell; RH, percent relative hemolysis; 5-SASL, 5-doxyl stearic acid spin label; Triton X-100 or TTX-100, t-Octylphenoxypolyethoxyethanol

* Corresponding author. Department of Biochemistry, Institute of Biology, UNICAMP, C.P. 6109 CEP 13083-970, Campinas, SP, Brazil. Tel.: +55 19 35216143; fax: +55 19 35216129.
E-mail address: depaula@unicamp.br (E. de Paula).

0005-2736/$ – see front matter © 2010 Elsevier B.V. All rights reserved.
doi:10.1016/j.bbamem.2010.10.016

micelles grow gradually richer in detergent. In the model proposed by Le Maire et al. [6], solubilization involves a number of intermediary states; it usually starts by destabilization of the lipid component of the membranes, a process that is accompanied by a transition of detergent binding by the membrane from a noncooperative to a cooperative interaction, already below the critical micelle concentration (CMC). This leads to the formation of membrane fragments with detergent-shielded edges.

In recent years, it has been found that certain lipids (sphingolipids and cholesterol) and protein (e.g., glycosylphosphatidylinositol-anchored proteins) components of biological membranes are resistant to detergent extraction, in particular TTX-100, giving rise to so-called detergent-resistant membranes (DRMs) [7–9]. These lipid-rich complexes have been also reported in erythrocytes [10–15] and are postulated to be involved in membrane-mediated events such as endocytosis of pathogens into cells, signal transduction, cholesterol trafficking, spermatozoa capacitation [16–19]. The selective uptake of detergent-resistant membrane proteins and cytoplasmic remodeling of membrane components was demonstrated in erythrocytes during malarial infection [20].

TTX-100 is a nonionic detergent, commonly used in studies of biomembranes [21–26]. The solubilization of lipid membranes triggered by TTX-100 is a well-described phenomenon [27,28]. The hemolytic action of this detergent has also been widely studied [8,24–26,29,30]. We have published a quantitative analysis of the hemolytic effect of TTX-100 on human erythrocyte membranes [31] employing the model described by Lichtenberg [32], using very low membrane concentrations.

Among the approaches used in the study of detergent–membrane interactions, spectroscopic techniques have been largely employed [33]. Spin labeling EPR has been one of the most important spectroscopic tools in providing information about molecular order and dynamics in bilayers [34–36] and micelles [37]. Spin label spectra are highly sensitive to effects on molecular organization caused by the partitioning of solutes into bilayers [38–40] and have been used to investigate the interaction between detergents and model or biological membranes [2,29–41], as well as protein-detergent interactions [30,42]. These studies showed that detergent incorporation into the bilayer decreases the molecular order and increases the mobility of the phospholipid hydrocarbon chains [2,41,43–46]. Moreover, spectra of spin-labeled fatty acids were used to distinguish the packing properties of DRMs from those of intact erythrocyte membranes [12,15,47]. However, no study making use of spin labeling EPR has dealt with the whole ensemble of events involved in detergent–membrane interaction.

Here we present a comprehensive study of the effect of TTX-100 upon membranes of human erythrocytes, encompassing a broad range of D/L, at detergent concentrations varying from below to above the CMC. Assessment of hemolysis by determination of Hb and inorganic phosphate, and analysis of EPR spectra of a fatty acid spin probe (5-doxyl stearic acid, 5-SASL) incorporated in whole cell suspensions, pellets and supernatants allowed the evaluation of the D/L at which membrane permeability was affected, as well as the characterization of the structures present at different D/L.

2. Materials and methods

2.1. Chemicals

5-SASL and TTX-100 were from Sigma Chemical Co. All other reagents were of analytical grade.

2.2. Hemolytic assay and phosphate determination

Human blood was freshly collected in a blood bank (Hemocentro/Unicamp). Erythrocytes were obtained by centrifuging three times at 1000*g* for 3 min with 5 mM phosphate buffered saline (PBS), pH 7.4. Variable TTX-100 concentrations were added to the erythrocyte suspensions to a final hematocrit (Ht) of 40% and the samples were kept for 15 min at 37 °C. After centrifugation at 10,000*g* for 3 min, the concentration of hemoglobin (Hb) released in the supernatant was measured at 412 nm, as described before [48]. In a similar way, the intracellular phosphate released in the supernatant was determined as inorganic phosphate, according to Chen et al. [49], after subtraction of the amount of phosphate present in PBS. The extent of hemolysis, expressed as relative hemolysis (RH), was determined on the basis of released Hb or phosphate in the supernatant, according to Eq. (1) [48]:

$$RH = \frac{A_s - A_{c1}}{A_{c2} - A_{c1}} \times 100 \quad (1)$$

where A_s, A_{c1}, and A_{c2} are the absorbance at 412 nm of the sample, the mechanical hemolysis control (erythrocytes in PBS), and the 100% hemolysis control (erythrocytes in water), respectively. Each experiment was run in triplicate; RH values represent the mean of three independent experiments.

2.3. EPR studies of TTX-100 micelles

Films of 5-SASL were prepared by evaporating a stock chloroform solution of the spin label under a stream of N_2. The remaining solvent was removed under vacuum for 2 h. PBS buffer was added to produce a final concentration of 1.10^{-5} M 5-SASL and the samples were vortexed for about 5 min. Aliquots of a TTX-100 stock solution were added in order to obtain a range of detergent concentrations. EPR spectra were recorded in 0.2 mL flat quartz cells (Wilmad Glass Co., Buena, NJ), at room temperature (22 ± 2 °C), in a Bruker EMX spectrometer, operating at 9 GHz and 3.4 kG.

2.4. EPR studies of erythrocytes

5-SASL films were prepared as described above and erythrocytes (80% Ht) were added so that the final spin label concentration did not exceed 2 mol% of erythrocyte membrane lipid [40]. The samples were gently shaken for 15 min at 37 °C, TTX-100 was added to the erythrocyte suspensions to reach a final Ht of 40%, and the samples were kept for 15 min at 37 °C. EPR spectra were obtained at room temperature (22 ± 2 °C) for the whole erythrocyte suspensions (before centrifugation), and for the supernatants and pellets (after centrifugation at 10,000*g* during 3 min) as described above.

2.5. Analysis of EPR spectra: calculation of the order parameter

The orientation of the lipid long molecular axis with respect to the bilayer normal can be evaluated by calculating the order parameter *S*, from the EPR spectra of a reporter molecule (spin label) inserted in the membrane [34]. *S* reflects the angular amplitude of anisotropic motion of the reporter molecule and is determined making use of Eq. (2):

$$S = \frac{2A_{//} - 2A_{\perp}}{2\left[A_{zz} - \left(A_{xx} + A_{yy}\right)/2\right]} \quad (2)$$

where $2A_{//}$ and $2A_{\perp}$ are the separations between the outer and inner extrema, respectively, in the experimental spectrum (these features are clearly seen in Fig. 2A). $A_{//}$ ($A_{\perp}$) is the hyperfine splitting corresponding to spin labels whose long molecular axes are oriented approximately parallel (perpendicular) to the external magnetic field. A_{xx}, A_{yy}, and A_{zz} are the values of the principal components of the hyperfine tensor (A_{zz} = 32.0 G, $A_{xx} = A_{yy}$ = 6.0 G) [35]. For stearic acid spin labels the long molecular axis is approximately parallel to the nitroxide *z* axis

(the direction of the pπ orbital that contains the unpaired electron), the *x* axis is parallel to the N—O bond, and the *y* axis is perpendicular to *x* and *z*. The larger the value of *S*, the smaller the amplitude of motion and the more ordered the lipid chains. *S* varies from 0 (in isotropic systems) to 1 (for a perfectly oriented molecule) [35]. Corrections for $A_{\perp}$ and for polarity were not included in the equation.

3. Results

3.1. Release of hemoglobin and intracellular phosphate to the supernatant

Fig. 1 presents the curves corresponding to Hb and inorganic phosphate released from erythrocyte suspensions (40% Ht) under isotonic conditions, pH 7.4, as a function of TTX-100 concentration. Both were determined in supernatants after sample centrifugation. Taking the Hb results, the curve can be divided into four regions: (i) between 0.1 and 0.3 mM TTX-100, where RH raises slowly with increasing detergent concentration, (ii) between 0.3 and 0.7 mM TTX-100 where the slope is much greater, (iii) between 0.7 and 1.0 mM TTX-100 where the curve raises very steeply, and finally, (iv) above 1.0 mM TTX-100, where hemolysis reaches 100%. We have ascribed the concentration of 0.3 mM TTX-100 to the beginning of the hemolytic process. The appearance of inorganic phosphate in the supernatant follows a very similar pattern, although Pi release began at lower detergent concentrations than those required for the beginning of release of Hb.

3.2. Spin label study of TTX-100 micelles

Fig. 2 shows the EPR spectra of 5-SASL in the presence of variable TTX-100 concentrations. From top to bottom of Fig. 2A, spectra of the label are seen in solution (PBS buffer) and at increasing (0.1–50 mM) TTX-100 concentrations. The spectrum in solution is typical of a probe tumbling freely in solution. As the detergent concentration increases, spectra due to motionally restricted label appear. The appearance of such spectra occurs in the concentration range of the CMC (0.23–0.3 mM) of TTX-100 [50]. For concentrations between 0.4 and 0.7 mM, the spectra due to more immobilized label do not display outer and inner extrema and evince some exchange broadening (see spectrum for 0.5 mM TTX-100). The spectra also show that at the lower detergent concentrations, 5-SASL partitions between the aqueous phase and the micelles. As the detergent concentration increases, the spin label increasingly partitions into the micelle, until no more label is detectable in the aqueous phase. Inner and outer extrema could be measured at 0.8 mM TTX-100 and above (Fig. 2A), allowing for the calculation of the order parameter, *S*. The appearance of inner and outer extrema is in contrast with data reported for other well known micellar systems [37,51] for which the lack of these features in the spectra has been ascribed to the small micelles size and the fast tumbling of the molecules within the aggregate, but it has been detected in micelles with large aggregation numbers such as that of the zwitterionic amidosulfobetaine (ASB) detergents [52].

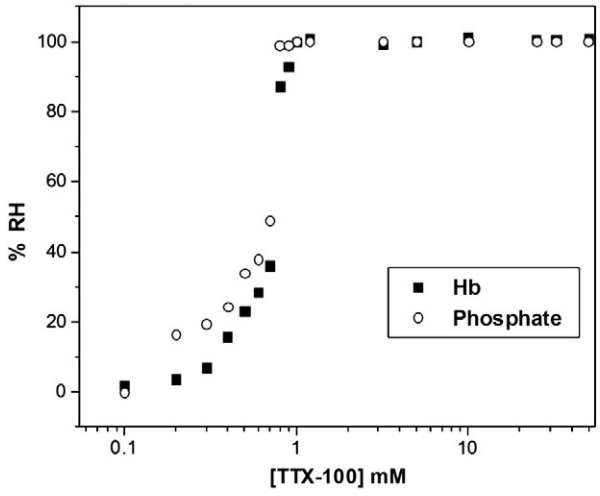

Fig. 1. Hemolytic effect of TTX-100 on human erythrocytes at 40% Ht, in 5 mM PBS buffer, pH 7.4, after incubation at 37 °C for 15 min, as measured by release of hemoglobin (■) or inorganic phosphate (○) in the supernatant. Results are representative of 3 independent experiments.

The presence of inner and outer extrema in the spectra of 5-SASL incorporated in TTX-100 micelles indicates that these aggregates are larger and/or more tightly packed than previously studied micelles. Indeed, in studies of TTX-100 micelles, Robson and Dennis have suggested that they consist of oblate ellipsoid aggregates with semiaxes of 2.7 and 5.2 nm [50]. The particle's rotational correlation time, τ, was calculated making use of the Stokes–Einstein equation (Eq. (3))

$$\tau = \frac{4\pi r 3\eta}{3\kappa T} \tag{3}$$

where r, η, k, and T are the particle radius, viscosity, Boltzmann constant, and temperature, respectively. Assuming that $r = 4.0$ nm (the average of 2.7 nm and 5.2 nm) one obtains $\tau = 5.1 \times 10^{-8}$ s. This value corresponds to a tumbling rate slow in the timescale of the EPR experiment and indicates that the motion reported in the spectra is that of the spin label within the micellar particle. Such value would give rise to a powder spectrum, which is not observed. Thus, the motion reported by the spectra corresponds to that of the probe within the micellar particle; this motion is restricted enough to give rise to spectra displaying outer and inner extrema (Fig. 2A). Very likely, the chemical structure of the nonionic detergent contributes to a tighter packing than in smaller, ionic detergent micelles. However, the order parameters calculated for these spectra are much smaller than those observed for whole RBC suspensions, pellets, and supernatants (Table 1).

3.3. Spin label study of detergent-erythrocyte interaction

In order to investigate the structural properties of the various aggregates resulting from the interaction of erythrocytes at 40% hematocrit with variable TTX-100 concentrations, the lipid spin probe 5-SASL was incorporated in RBC and EPR spectra were obtained for whole cell suspensions, pellets and supernatants. The amphiphilic character of the spin probe drives its intercalation between the molecular components of aggregates such as micelles and bilayers.

Fig. 2B presents the EPR spectra of 5-SASL in whole RBC suspensions after treatment with variable TTX-100 concentrations (left), as well as their respective supernatants (center), and pellets (right). This figure shows that at the lower detergent concentrations, the pellets spectral intensity corresponds to the majority of the label population. This population decreases stepwise up to 0.6 mM detergent and is not detectable at 0.9 mM and higher TTX-100 concentrations. In contrast, the spectra corresponding to supernatant display very weak intensity up to 0.6 mM TTX-100, suggesting that at low detergent concentration this population is very small. The situation is reversed for higher detergent concentrations. At 0.9 mM TTX-100 and above, while essentially no pellet spectrum is detected, the supernatants display spectra with much higher intensity than at the lower detergent concentrations. It is noteworthy that 0.9 mM is the detergent concentration at which Hb and intracellular inorganic phosphate release are finished (Fig. 1).

Table 1 presents the values of order parameters calculated for the spectra of 5-SASL in whole RBC suspensions, supernatants, pellets, and pure TTX-100 micelles. For the RBC suspensions in the presence of

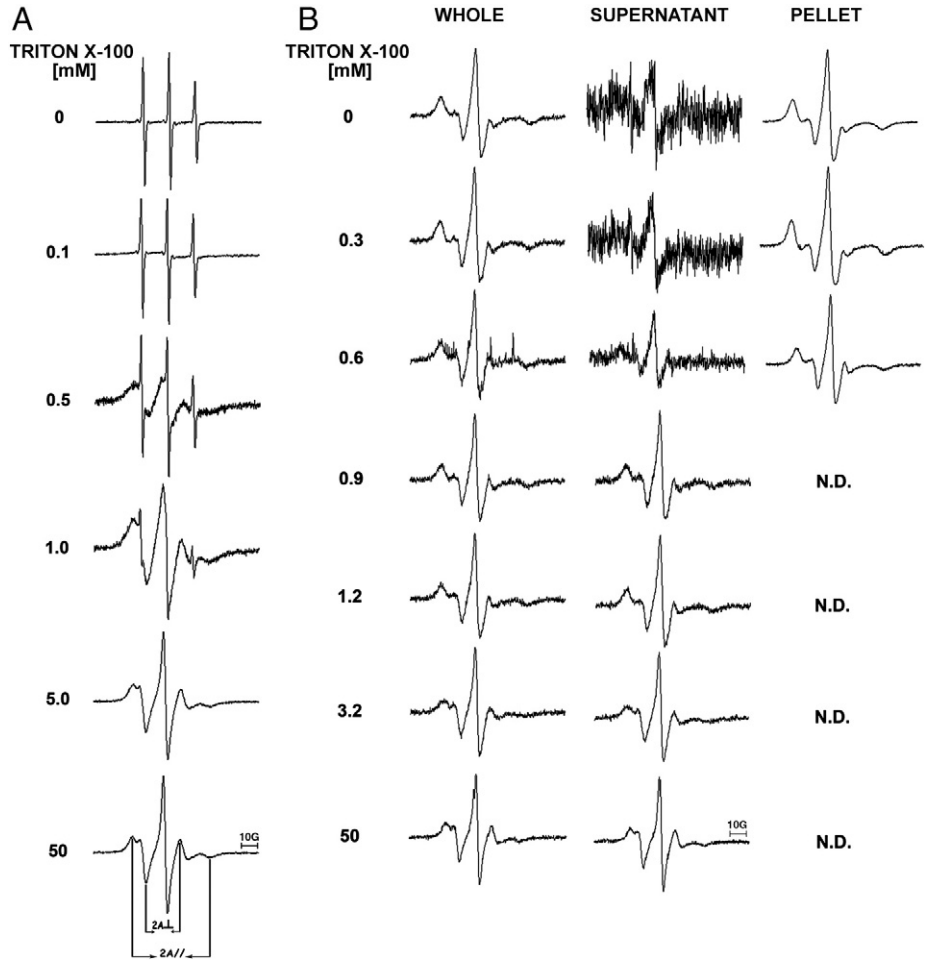

Fig. 2. EPR spectra of 5-SASL at increasing TTX-100 concentrations (0–50 mM): A) in PBS buffer; B) in 40% Ht erythrocyte membranes: whole suspension (left column), supernatant (central) and pellet (right column). N.D. = not determined (see text).

Table 1
Order parameter, *S*, calculated for the spectra of 5-SASL incorporated in whole erythrocytes, supernatant, and pellet in the presence of increasing TTX-100 concentrations. The last column gives the values of *S* for pure TTX-100 solutions[a].

[TTX-100] mM		Red blood cells		
	S TTX-100	*S* Whole	*S* Supernatant	*S* Pellet
0.0	Nd[b]	0.697	Nd[c]	0.700
0.1	Nd[b]	0.710	Nd[c]	0.707
0.2	Nd[b]	0.700	Nd[c]	0.699
0.3	Nd[b]	0.711	Nd[c]	0.695
0.4	Nd[d]	0.689	Nd[c]	0.695
0.5	Nd[d]	0.670	0.702	0.693
0.6	Nd[d]	0.667	0.691	0.681
0.7	Nd[d]	0.670	0.695	Nd[e]
0.8	0.482	0.677	0.701	Nd[e]
0.9	0.447	0.671	0.689	Nd[d]
1.0	0.449	0.672	0.669	Nd[d]
1.2	0.478	0.667	0.650	Nd[d]
2.5	0.448	0.670	0.639	Nd[d]
3.2	0.448	0.614	0.619	Nd[d]
10.0	0.466	0.519	0.528	Nd[d]
25.0	0.461	0.498	0.498	Nd[d]
32.5	0.458	0.490	0.486	Nd[d]
50.0	0.461	0.472	0.479	Nd[d]

[a] Experimental conditions as in Fig. 2.
[b] Only the spectrum due to label free in solution was detected.
[c] Not determined, because of high noise in the spectra due to the small amount of aggregates in the supernatant.
[d] Not determined, see text.
[e] Spectra were not obtained because the volumes of the remaining pellet fractions were too small.

variable detergent concentration, three different regions can be distinguished: (i) between 0 and 0.4 mM detergent, where the values of *S* ranged from 0.689 to 0.711 for whole RBC suspensions. Very similar values were obtained for the pellets (0.695–0.707), suggesting that incorporation of the detergent did not cause a significant effect on bilayer organization. In this region the supernatants yielded essentially undetectable spectra (ii) between 0.5 and 0.9 mM detergent, where *S* for whole RBC suspensions ranged between 0.667 and 0.677, while the supernatants yielded somewhat higher, also approximately constant, *S* values (0.689–0.702). Spectra of the pellets were detectable for 0.5 and 0.6 mM TTX-100, however, the amounts of pellet for 0.7 and 0.8 mM TTX-100 were not sufficient to obtain EPR spectra; (iii) 1.0 mM TTX-100 and above: the values of *S* decreased and were very similar for both whole RBC suspensions and supernatants. In this concentration range essentially no pellet was detected; therefore, the whole RBC suspensions and supernatants were essentially equivalent. At the highest detergent concentrations (25 mM and above) the spectra, and consequently, the values of *S* approached those of pure TTX-100 micelles.

A plot of *S* as a function of TTX-100 concentration is given in Fig. 3. The figure shows that the order parameter decreased to a small extent up to approximately 2.5 mM detergent, and started to decrease more steeply at 3.2 mM TTX-100, reaching a much lower value at 10 mM detergent. Between 10 mM and 50 mM detergent, *S* decreased in a less pronounced manner and the EPR spectra approached that of pure TTX-100 micelles. This behavior was very similar for both whole RBC suspensions and supernatants. *S* values obtained for pure TTX-100 samples are also plotted. In addition, the EPR data are compared to the

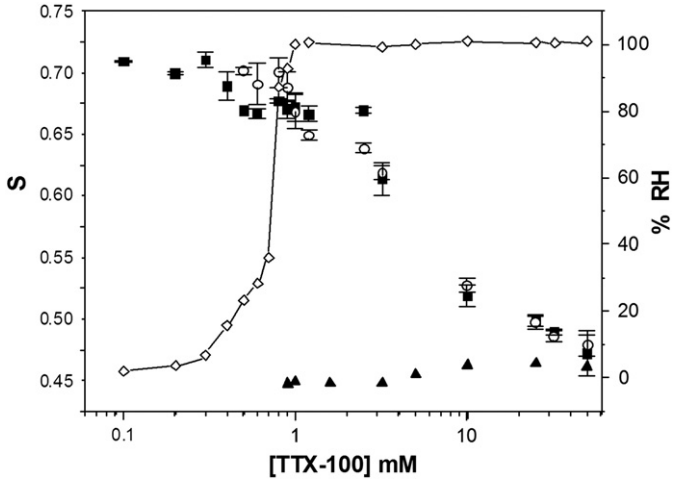

Fig. 3. Relative hemolysis (◊) and order parameters for whole human RBC suspension (40% Ht, in 5 mM PBS buffer, pH 7.4, 22 ± 2 °C) (■) and supernatants (○) as a function of TTX-100 concentration. Error bars represent the standard deviation ($n = 3$). *S* values for 5-SASL spectra in pure TTX-100 solutions (▲) are also plotted.

relative hemolysis as a function of detergent concentration (right axis). Fig. 3 clearly shows that both parameters do not display a parallel behavior.

4. Discussion

Several models have been proposed for the steps involved in the process of membrane solubilization by detergent. On the basis of previous suggestions by Helenius and Simons [53], Lichtenberg proposed a mechanism describing the process as a membrane-to-micelle transition [4,32] with the transient formation of both mixed membranes and mixed micelles, composed by lipids, proteins, and detergent molecules. In this model, the detergent is proposed to partition into the bilayer until reaching a saturating detergent/lipid molar ratio (D/L). At higher D/L, mixed lipid–detergent bilayers coexist with mixed detergent-lipid micelles. Further increase of detergent leads to increased membrane solubilization with formation of detergent micelles with increasing D/L. Goñi and coworkers used this approach to study the solubilization of lipid and biological membranes by different nonionic detergents [27,54,55].

In previous work [31], we examined the interaction between TTX-100 and membranes of human erythrocytes when intact RBC were exposed to increasing detergent concentrations. These studies were performed at lower membrane concentrations (0.075 to 0.45% Ht) than in the present work. The beginning and end of hemolysis were taken as an indication of the achievement of bilayer saturation by the detergent and the end of membrane solubilization, respectively. However, at such low membrane concentrations, it was not possible to investigate the structures of the aggregates formed in the presence of the various detergent concentrations.

Other models have been proposed to describe the mechanism of membrane–detergent interaction. Lasch and coworkers [5,56] and Moller and coworkers [6,57] have reported the formation of membrane fragments in the initial stages of solubilization, and proposed that that detergent molecules would be located at the edges of these fragments, shielding the hydrophobic portions of lipids and proteins from the contact with the aqueous solvent. Indeed, membrane sheets have been detected in studies of the interaction of detergents with model systems containing pure lipids [58] as well as lipid and protein [57] with detergents.

In the present study, the goal was to make use of spin label spectra in order to characterize the structural and dynamic properties of aggregates formed upon the interaction between TTX-100 and human erythrocyte membranes when intact RBC are exposed to increasing detergent concentrations. Since the spin labeling technique requires membrane concentrations much higher than those used in our previous study [31], it was possible to examine the various types of aggregates formed during the different stages of membrane–detergent interaction. The results showed that under the conditions used in the present work, a more complex picture emerges, as evidenced by the following observations: The hemolysis study showed that this process started and ended at approximately 0.3 and 0.9 mM TTX-100, respectively (Fig. 1). These concentrations correspond to D/L of approximately 0.08 and 0.26; these values are much smaller than those found previously for the onset and end of membrane solubilization in phospholipid bilayers: 0.7 and 3.0, respectively [27] or 0.64 and 2.5, respectively [59].

Interestingly, the EPR spectra indicated that at 0.9 mM detergent, essentially no pellet was present in the sample, and, therefore, the whole population of RBC suspensions at this and higher TTX-100 concentrations was found in the supernatants. Moreover, the presence of low intensity signals in the supernatants started at concentrations as low as 0.3 mM TTX-100, increasing considerably up to 0.9 mM detergent (Fig. 2B and Table 1). An examination of the variation of the order parameter (Table 1 and Fig. 3) reveals that the values of *S* decreased very slowly between 0.1 and 2.5 mM TTX-100 and were similar for whole cell suspensions, pellets and supernatants. Thus, the aggregates in the supernatant in this range of detergent concentration display molecular packing properties very similar to those of the native membranes.

A steeper decline in the values of *S* occurred between 2.5 and 10 mM TTX-100, and a slower decrease up to 50 mM detergent, reaching those of the pure detergent micelles (Fig. 3 and Table 1). The concentrations of 2.5 mM and 10 mM correspond to D/L of 0.72 and 2.88, which is in the range of those reported for membrane saturation and solubilization in pure lipid bilayers [27,59,60].

How can these findings be interpreted? We propose that the initial incorporation of TTX-100 into the bilayer leads to an increase in permeability which, due to a colloid osmotic imbalance, causes formation of pores of size sufficient to allow the release of hemoglobin. Previous studies of detergent–membrane interaction have demonstrated that detergent intercalation into intact membranes causes an increase in permeability prior to the beginning of solubilization [55,59]. Chernitsky and Senkovich [61] have evaluated that the diameter of detergent-induced pores in erythrocytes is of the order of 4 nm. The size of Hb is 5.5 nm [62], thus it is quite plausible that the protein could exit through these pores, at D/L lower than those necessary for the actual membrane solubilization.

The presence of spectra resembling those of the native membrane in the supernatant in the concentration range 0.1–2.5 mM TTX-100 (Fig. 2B) suggests the formation of membrane fragments (or vesicles) small enough to remain in suspension upon centrifugation. This hypothesis is corroborated by the similarity of *S* values for whole cell suspensions and supernatants (Fig. 3 and Table 1). This picture is in agreement with work on the solubilization of membranes containing the Ca^{2+}-ATPase, where the authors describe the appearance of different aggregates prior to solubilization [57]. It is noteworthy that a greater variety of stages (and aggregates) was found with TTX-100. The authors proposed a model for non-cooperative detergent insertion in the bilayer to account for changes in bilayer molecular packing and, therefore, permeability, and for cooperative formation of edges, creating the curvature that would allow the formation of fragments of limited size.

The presence of membrane fragments in the supernatant at low D/L is clearly evinced in the present study. Although the noise in the spectra does not allow the measurement of outer and inner extrema with good accuracy, Table 1 shows that the membrane fragments in the supernatants, especially at the lower detergent concentrations, posses somewhat higher order parameters than the pellets and/or whole cells, suggesting that the fragments could be enriched in cholesterol and sphingolipids. It is noteworthy that DRMs are described as enriched in those lipids [9]. Actually, DRMs from human erythrocyte ghosts

obtained in particular conditions (under centrifugation in a sucrose gradient at 4 °C), contain around 30% of total membrane cholesterol [13] and we have recently reported an increase in *S* values of these erythrocyte membrane fragments prepared with TTX-100 (in comparison to native RBC) that has been ascribed to the formation of a liquid-ordered, cholesterol-enriched phase at both 4 °C [15] and 37 °C [63].

The membrane-like fragments persist up to 2.5 mM detergent (D/L 0.72). Subsequently, as the detergent concentration increases, membrane solubilization effectively occurs. As D/L increases, detergent micelles containing low proportions of lipid and/or protein prevail and approach the composition and molecular organization of pure detergent micelles. This is also evinced by the EPR spectra (compare Fig. 2A and B) and by the values of order parameters (Table 1 and Fig. 3). Fig. 3 shows that the order parameter decreases steeply between 2.5 and 10.0 mM TTX-100, and that the decrease of this parameter is slow for higher detergent concentrations up to 50.0 mM. Interestingly the D/L ratio at 10.0 mM TTX-100 is 2.88. Thus, although a more complex series of events was observed in the present study, the stage of conversion from membrane to mixed micelles seems to occur at D/L ratios close to those observed in model membranes.

In conclusion, the results indicate the interaction between whole RBC and TTX-100 consists of an ensemble of stages: the initial incorporation of detergent molecules into the membrane leads to a decrease in molecular packing which causes an increase in permeability, resulting in hemolysis. Subsequently, EPR spectra of an intercalated spin probe in the supernatant phase revealed the presence of detergent-stabilized membrane fragments, probably by means of edges surrounding these fragments. Finally, at higher detergent concentrations, full membrane solubilization is achieved, its molecular components being incorporated into detergent micelles. Thus, EPR spectra, in conjunction with hemolysis data, allowed the characterization of the various structures formed in the different stages of detergent–membrane interaction.

Acknowledgments

This research was supported by grants from FAPESP to SS and EP. PSCP was recipient of a Ph.D. fellowship from CAPES. SS and EP are CNPq research fellows.

References

[1] D. Attwood, A.T. Florence, Surfactant Systems, their Chemistry, Pharmacy and Biology, 2nd ed., Chapman & Hall, London, New York, 1983.
[2] R.E. Glover, R.R. Smith, M.V. Jones, S.K. Jackson, C.C. Rowlands, An EPR investigation of detergent action on bacterial membranes, FEMS Microbiol. Lett. 177 (1999) 57–62.
[3] D. Linke, Detergents: an overview, Meth. Enzymol. 463 (2009) 603–617.
[4] D. Lichtenberg, E. Opatowski, M.M. Kozlov, Phase boundaries in mixtures of membrane-forming amphiphiles and micelle-forming amphiphiles, Biochim. Biophys. Acta 1508 (2000) 1–19.
[5] J. Lasch, Interaction of detergents with lipid vesicles, Biochim. Biophys. Acta 1241 (1995) 269–292.
[6] M. Le Maire, P. Champeil, J.V. Moller, Interaction of membrane proteins and lipids with solubilizing detergents, Biochim. Biophys. Acta 1508 (2000) 86–111.
[7] D.A. Brown, J.K. Rose, Sorting of GPI-anchored proteins to glycolipid-enriched membrane subdomains during transport to the apical cell surface, Cell 68 (1992) 533–544.
[8] L.H. Chamberlain, Detergents as tools for the purification and classification of lipid rafts, FEBS Lett. 13 (559) (2004) 1–5.
[9] L.J. Pike, Lipid rafts: heterogeneity on the high seas, Biochem. J. 378 (2004) 281–292.
[10] B.U. Samuel, N. Mohandas, T. Harrison, H. McManus, W. Rosse, M. Reid, K. Haldar, The role of cholesterol and glycosylphosphatidylinositol-anchored proteins of erythrocyte rafts in regulating raft protein content and malarial infection, J. Biol. Chem. 276 (2001) 29319–29329.
[11] U. Salzer, R. Prohaska, Stomatin, flotillin-1, and flotillin-2 are major integral proteins of erythrocyte lipid rafts, Blood 97 (2001) 1141–1143.
[12] M.G. Rivas, A.M. Gennaro, Detergent resistant domains in erythrocyte membranes survive after cell cholesterol depletion: an EPR spin label study, Chem. Phys. Lipids 122 (2003) 165–169.
[13] A. Ciana, C. Balduini, G. Minetti, Detergent-resistant membranes in human erythrocytes and their connection to the membrane-skeleton, J. Biosci. 30 (2005) 317–328.
[14] K. Kamata, S. Manno, M. Ozaki, Y. Takakuwa, Functional evidence for presence of lipid rafts in erythrocyte membranes: Gsα in rafts is essential for signal transduction, Am. J. Hematol. 83 (2008) 371–375.
[15] C. Crepaldi Domingues, A. Ciana, A. Buttafava, C. Balduini, E. de Paula, G. Minetti, Resistance of human erythrocyte membranes to Triton X-100 and $C_{12}E_8$, J. Membr. Biol. 227 (2009) 39–48.
[16] S. Manes, G. del Real, A.C. Martinez, Pathogens: raft hijackers, Nat. Rev. Immunol. 3 (2003) 557–568.
[17] K. Simons, R. Ehehalt, Cholesterol, lipid rafts, and disease, J. Clin. Invest. 110 (2002) 597–603.
[18] K.A.G. Yoneyama, A.K. Tanaka, T.G.V.H. Silveira, K. Takahashi, A.H. Straus, Characterization of Leishmania (Viannia) braziliensis membrane microdomains, and their role in macrophage infectivity, J. Lipid Res. 47 (2006) 2171–2178.
[19] B. Nixon, R.J. Aitken, The biological significance of detergent-resistant membranes in spermatozoa, J. Reprod. Immunol. 83 (2009) 8–13.
[20] S.C. Murphy, S. Fernandez-Pol, P.H. Chung, S.N.P. Murthy, S.B. Milne, M. Salomao, H.A. Brown, J.W. Lomasney, N. Mohandas, K. Haldar, Cytoplasmic remodeling of erythrocyte raft lipids infection by the human malaria parasite *Plasmodium falciparum*, Blood 110 (2007) 2132–2139.
[21] J.I.G. Gurtubay, F.M. Goñi, J.C. Gómez-Fernández, J.J. Otamendi, J.M. Macarulla, Triton X-100 solubilization of mitochondrial inner and outer membranes, J. Bioenerg. Biomembr. 12 (1980) 47–70.
[22] M.P. Molloy, B.R. Herbert, B.J. Walsh, M.L. Tyler, M. Traini, J.C. Sanchez, D.F. Hochstrasser, K.L. Williams, A.A. Gooley, Extraction of membrane proteins by differential solubilization for separation using two-dimensional gel electrophoresis, Electrophoresis 19 (1998) 837–844.
[23] J.G. Okun, V. Zickermann, K. Zwicker, U. Brandt, Binding of detergents and inhibitors to bovine complex I—a novel purification procedure for bovine complex I retaining full inhibitor sensitivity, Biochim. Biophys. Acta 1459 (2000) 77–87.
[24] J. Bielawski, Two types of haemolytic activity of detergents, Biochim. Biophys. Acta 1035 (1990) 214–217.
[25] J. Bielawski, L. Mrówczynska, M. Konarczak, Hemolytic activity of the non-ionic detergents Tween 80 and Triton X-100, Biol. Bull. Poznan 32 (1995) 27–41.
[26] D. Trägner, A. Csordas, Biphasic interaction of Triton detergents with the erythrocyte membrane, Biochem. J. 244 (1987) 605–609.
[27] M.A. Partearroyo, M.A. Urbaneja, F.M. Goñi, Effective detergent/lipid ratios in the solubilization of phosphatidylcholine vesicles by Triton X-100, FEBS Lett. 302 (1992) 138–140.
[28] A. de La Maza, J.L. Parra, M.T. Garcia, I. Ribosa, J.S. Leal, Permeability changes in the phospholipid bilayer caused by nonionic surfactants, J. Colloid Interface Sci. 148 (1992) 310–316.
[29] M.N. Jones, Surfactants in membrane solubilisation, Int. J. Pharm. 177 (1999) 137–159.
[30] N.B. Bam, T.W. Randolph, J.L. Cleland, Stability of protein formulations: Investigation of surfactant effects by a novel EPR spectroscopic technique, Pharm. Res. 122 (1995) 2–11.
[31] P.S.C. Preté, S.V.P. Malheiros, N.C. Meirelles, E. de Paula, Quantitative assessment of human erythrocyte membrane solubilization by Triton X-100, Biophys. Chem. 97 (2002) 1–5.
[32] D. Lichtenberg, Characterization of the solubilization of lipid bilayers by surfactants, Biochim. Biophys. Acta 821 (1985) 470–478.
[33] F.M. Goñi, A. Alonso, Spectroscopic techniques in the study of membrane solubilization, reconstitution and permeabilization by detergents, Biochim. Biophys. Acta 1508 (2000) 51–68.
[34] W.L. Hubbell, H.M. McConnell, Molecular motion in spin-labeled phospholipids and membranes, J. Am. Chem. Soc. 93 (1971) 314–326.
[35] S. Schreier, C.F. Polnaszek, I.C.P. Smith, Spin labels in membranes, Biochim. Biophys. Acta 515 (1978) 375–436.
[36] D. Marsh, Spectroscopic studies of membrane structure, Essays Biochem. 11 (1975) 139–180.
[37] S. Schreier, J.R. Ernandes, I.M. Cuccovia, H. Chaimovich, Spin label studies of structural and dynamic properties of detergent aggregates, J. Magn. Reson. 30 (1978) 283–298.
[38] S. Schreier, W.A. Frezzatti, P.S. Araujo, H. Chaimovich, I.M. Cuccovia, Effect of lipid membranes on the apparent pK of the local anesthetic tetracaine. Spin label and titration studies, Biochim. Biophys. Acta 769 (1984) 231–237.
[39] E. Lissi, M.L. Bianconi, A.T. Amaral, E. de Paula, L.E.B. Blanch, S. Schreier, Methods for the determination of partition coefficients based on the effect of solutes upon membrane structure, Biochim. Biophys. Acta 1021 (1990) 46–50.
[40] E. de Paula, S. Schreier, Use of a novel method for determination of partition coefficients to compare the effect of local anesthetics on membrane structure, Biochim. Biophys. Acta 1240 (1995) 25–33.
[41] J. Mizushima, Y. Kawasaki, T. Tabohashi, T. Kitano, K. Sakamoto, M. Kawashima, R. Cooke, H.I. Maibach, Effect of detergents on human stratum corneum: electron paramagnetic resonance study, Int. J. Pharm. 197 (2000) 193–202.
[42] L.S. Jones, D. Cipolla, J. Liu, S.J. Shire, T.W. Randolph, Investigation of protein–surfactant interactions by analytical ultracentrifugation and electron paramagnetic resonance: the use of recombinant human tissue factor as an example, Pharm. Res. 16 (1999) 808–812.
[43] F. Sersen, A. Leitmanová, F. Devínsky, I. Lacko, P. Balgavy, A spin label study of perturbation effects of N-(1-methyldodecyl)-N, N, N-trimethylammonium bromide and N-(1-methyldodecyl)-N, N-dimethylamine oxide on model membranes prepared from *Escherichia coli*-isolated lipids, Gen. Physiol. Biophys. 8 (1989) 133–156.
[44] E. Galembeck, A. Alonso, N.C. Meirelles, Effects of polyoxyethylene chain length on erythrocyte hemolysis induced by poly[oxyethylene (n) nonylphenol] non-ionic surfactants, Chem. Biol. Interact. 113 (1998) 91–103.

[45] Y. Kawasaki, D. Quan, K. Sakamoto, H.I. Maibach, Electron resonance studies on the influence of anionic surfactants on human skin, Dermatology 194 (1997) 238–242.
[46] J. Gallová, F. Devínsky, P. Balgavy, Interaction of surfactants with model and biological membranes. II. Effect of N-alkyl-N, N, N-trimethylammonium ions on phosphatidylcholine bilayers as studied by spin probe ESR, Chem. Phys. Lipids 53 (1990) 231–241.
[47] P.M. Rodi, M.S. Cabeza, A.M. Gennaro, Detergent solubilization of bovine erythrocytes: comparison between the insoluble material and the intact membrane, Biophys. Chem. 122 (2006) 114–122.
[48] S.V.P. Malheiros, E. de Paula, N.C. Meirelles, Contribution of trifluoperazine/lipid ratio and drug ionization to hemolysis, Biochim. Biophys. Acta 1373 (1998) 332–340.
[49] P.S. Chen, T.Y. Toribara Jr., H. Warner, Microdetermination of phosphorus, Anal. Chem. 28 (1956) 1756–1758.
[50] R.J. Robson, E.A. Dennis, The size, shape and hydration of nonionic surfactant micelles of Triton X-100, J. Phys. Chem. 81 (1977) 1075–1078.
[51] J.R. Ernandes, H. Chaimovich, S. Schreier, Spin label study of detergents in the region of critical micelle concentration, Chem. Phys. Lipids 18 (1977) 304–315.
[52] C.C. Domingues, S.V.P. Malheiros, E. de Paula, Solubilization of human erythrocyte membranes by ASB detergents, Braz. J. Med. Biol. Res. 41 (2008) 758–764.
[53] A. Helenius, K. Simons, Solubilizaton of membranes by detergents, Biochim. Biophys. Acta 415 (1975) 29–79.
[54] A. Prado, J.L.R. Arrondo, A. Villena, F.M. Goñi, J.M. Macarulla, Membrane–surfactant interactions. The effect of Triton X-100 on sarcoplasmic reticulum vesicles, Biochim. Biophys. Acta 733 (1983) 163–171.
[55] M.B. Ruiz, A. Prado, F.M. Goñi, A. Alonso, An assessment of the biochemical applications of the non-ionic surfactant Hecameg, Biochim. Biophys. Acta 1193 (1994) 301–306.
[56] J. Lasch, J. Hoffman, W. Richter, H.W. Meyer, Structural perturbations of phospholipid bilayers induced by the neutral detergent octyl glucoside, J. Liposome Res. 2 (1992) 1–9.
[57] U. Kragh-Hansen, M. Le Maire, J.V. Moller, The mechanism of detergent solubilization of liposomes and protein-containing membranes, Biophys. J. 75 (1998) 2932–2946.
[58] M. Ollivon, O. Eidelman, R. Blumenthal, A. Walter, Micelle-vesicle transition of egg phosphatidylcholine and octyl glucoside, Biochemistry 27 (1988) 1695–1703.
[59] M.T. Paternostre, M. Roux, J. Rigaud, Mechanisms of membrane protein insertion into liposomes during reconstitution procedures involving the use of detergents. 1. Solubilization of large unilamellar liposomes (prepared by reverse-phase evaporation) by Triton X-100, octyl glucoside, and sodium cholate, Biochemistry 27 (1988) 2668–2677.
[60] F.M. Goñi, M.A. Urbaneja, J.L. Arrondo, A. Alonso, A.A. Durrani, D. Chapman, The interaction of phosphatidylcholine bilayers with Triton X-100, Eur. J. Biochem. 160 (1986) 659–665.
[61] E.A. Chernitsky, O.A. Senkovich, Erythrocyte hemolysis by detergents, Membr. Cell Biol. 11 (1997) 475–485.
[62] M.F. Perutz, The hemoglobin molecule, Sci. Am. 211 (1964) 64–76.
[63] C.C. Domingues, A. Cianna, A. Buttafava, B.R. Casadei, C. Balduini, E. de Paula, G. Minetti, Effect of cholesterol depletion and temperature on the isolation of detergent-resistant membranes from human erythrocytes, J. Membr. Biol. 234 (2010) 194–205.